Wetting of soap bubbles on hydrophilic, hydrophobic, and superhydrophobic surfaces

S. Arscott

Wetting of soap bubbles on hydrophilic, hydrophobic, and superhydrophobic surfaces

Cite as: Appl. Phys. Lett. **102**, 254103 (2013); https://doi.org/10.1063/1.4812710
Submitted: 22 March 2013 • Accepted: 13 June 2013 • Published Online: 27 June 2013

Steve Arscott

Wetting of soap bubbles on hydrophilic, hydrophobic, and superhydrophobic surfaces

Steve Arscott[a)]
Institut d'Electronique, de Microélectronique et de Nanotechnologie (IEMN), CNRS UMR8520, The University of Lille, Cité Scientifique, Avenue Poincaré, 59652 Villeneuve d'Ascq, France

(Received 22 March 2013; accepted 13 June 2013; published online 27 June 2013)

Wetting of sessile bubbles on various wetting surfaces (solid and liquid) has been studied. A model is presented for the apparent contact angle of a sessile bubble based on a modified Young's equation—the experimental results agree with the model. Wetting a hydrophilic surface results in a bubble contact angle of 90° whereas using a superhydrophobic surface one observes 134°. For hydrophilic surfaces, the bubble angle diminishes with bubble radius whereas on a superhydrophobic surface, the bubble angle increases. The size of the plateau borders governs the bubble contact angle, depending on the wetting of the surface. © *2013 AIP Publishing LLC*. [http://dx.doi.org/10.1063/1.4812710]

An understanding of the behavior of bubbles, liquid films, foams, and froths is vital for several fields including mining, manufacturing, materials, security, and food production,[1] and the use of soap bubbles and films has been recently demonstrated in micro[2,3] and nanotechnologies.[4,5] Soap bubbles and films have been studied for some time now;[6–9] more recent investigations include *inter alia* their composition,[10] organisation,[11,12] electrification,[13–15] magnetization,[16] wetting,[17–19] stability,[20] and mechanical[21] and optical properties.[22] Here, the wetting of sessile soap bubbles on solid surfaces (hydrophilic to superhydrophobic) and on a liquid surface is studied. The results have potential implications in the aforementioned applications.

Fig. 1 shows ideal cases for a sessile droplet wetting a solid surface [Fig. 1(a)], a sessile bubble wetting a solid surface [Fig. 1(b)], and a sessile bubble resting on the surface of a liquid [Fig. 1(c)]. For the droplet, the balance between the surface tension of the liquid γ_l, the solid-liquid γ_{sl}, and the solid-vapor γ_{sv} surface energies is given by Young's equation[23,24] and leads to a liquid contact angle θ_l

$$\gamma_{sv} = \gamma_l \cos\theta_l + \gamma_{sl}. \tag{1}$$

For a sessile bubble wetting a solid surface [Fig. 1(b)], Young's equation needs to be modified to take into account the internal surface of the bubble. As the bubble has two surfaces, its effective surface tension γ_b is twice the surface tension of the liquid, i.e., $\gamma_b = 2\gamma_l$. In addition to this, an extra γ_l term is required, acting in the same direction as γ_{sl}, in order to take into account creation of bubble surface inside the bubble. Thus, the modified Young's equation for an ideal sessile bubble forming a contact angle θ_{b0} with a solid surface can be written as

$$\gamma_{sv} = 2\gamma_l \cos\theta_{b0} + \gamma_l + \gamma_{sl}. \tag{2}$$

Equations (1) and (2) allow us to write the contact angle of an ideal sessile bubble θ_{b0} resting on a surface in terms of the contact angle of a droplet of bubble solution θ_l resting on the same surface

$$\cos\theta_{b0} = \frac{1}{2}(\cos\theta_l - 1). \tag{3}$$

Equation (3) assumes that the bubble film thickness at the bubble-solid interface is of the order of the liquid film forming the bubble and that the droplet and bubble are considered to be large enough so that the diminishing contact angle with droplet radius effect,[25] controversially attributed to the line tension,[24] is negligible. For a sessile bubble resting on the surface of a liquid of the same solution [Fig. 1(c)], if the Plateau borders are symmetrical[17] inside and outside the bubble and are much smaller than the bubble base radius, then the apparent contact angle $\theta_{b0} = 90°$ assuming the surface of the liquid to be perfectly hydrophilic, i.e., $\theta_l = 0$.

A commercially available soap solution (Pustefix, Germany) was used to generate bubbles for the experiments—a soap solution is a mixture of pure water, a second liquid to increase the viscosity of the solution and reduce drainage (e.g., glycerol), and a surfactant (e.g., an organosulphate). The surface tension of the solution was measured to be 28.2 mJ m^{-2} (standard deviation = 0.3 mJ m^{-2}) using the pendant drop method[26] and applying the appropriate correction factor (Ref. 27)—a value comparable with other experiments concerning soap bubbles and films.[13,17,18] As a calibration measurement, deionized water was measured, the result was a surface tension of 72.7 mJ m^{-2} (1.2). The density of the bubble solution was measured to be 997.8 kg m^{-3}.

The different wetting surfaces were fabricated using polished silicon wafers (Siltronix, France). In order of decreasing wetting, "Surface A" is a 200 nm thick layer of silicon dioxide grown on a silicon wafer using wet thermal oxidation. "Surface B" is a ~100 μm thick Polydimethylsiloxane (PDMS) layer—Sylgard® 184 (Dow Corning, USA) spin-coated onto a silicon wafer. "Surface C" is a ~250 nm Teflon® layer obtained using spin-coating of Teflon® AF 1600 (Dupont, USA) diluted with Fluorinert FC-75 (3M, USA).[28] "Surface D" is composed of "black silicon"[29] produced using dry etching. This surface was subsequently deposited with a ~20 nm thick fluorocarbon layer using a C_4F_8 plasma (STS, UK).

The measured contact angles θ_l of the soap solution on the surfaces A-D are given in the Table I. As the values of γ_{sv} are

a)Electronic mail: steve.arscott@iemn.univ-lille1.fr. Tel.: +33 320197979.

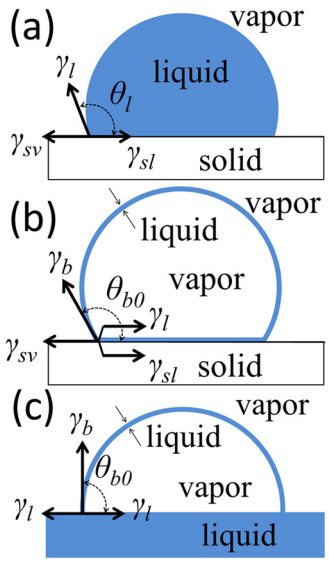

FIG. 1. Schematic diagrams showing the apparent contact angles for (a) a sessile droplet wetting a solid surface, (b) a sessile bubble wetting a solid surface, and (c) a sessile bubble resting on the surface of a liquid.

very well known for Teflon[24] ($15 \pm 2\,\mathrm{mJ\,m^{-2}}$) and PDMS[30] ($23.5 \pm 1.5\,\mathrm{mJ\,m^{-2}}$) we can determine the values of γ_{sl} to be ($1.8 \pm 2.5\,\mathrm{mJ\,m^{-2}}$) and ($6.5 \pm 2\,\mathrm{mJ\,m^{-2}}$). For a superhydrophobic surface, γ_{sv} is of the order of 5–10 $\mathrm{mJ\,m^{-2}}$ which indicates that γ_{sl} is in the range 15.5–20.5 $\mathrm{mJ\,m^{-2}}$. Bubbles having radii in the 0.5–10 mm range were generated for the experiments using a pipette (Bio-Rad, France) having a tip diameter of ~0.5 mm. All surface preparation and experiments were performed in a class ISO 5/7 clean room ($T = 20\,^{\circ}\mathrm{C} \pm 0.5\,^{\circ}\mathrm{C}$; $RH = 45\% \pm 2\%$). The data were gathered using a commercial Contact Angle Meter (GBX Scientific Instruments, France).

Bubbles were deposited onto surfaces A-D in order to form sessile bubbles [Fig. 2]. Millimeter-sized soap bubbles are quasi-spherical with radius of curvature R [Fig. 2(a)] and a contact angle θ_b [Fig. 2(b)] as the Bond number[24] is small. Drainage can cause the formation of liquid layer h (the Plateau border[9]) [Fig. 2(c)] at the bubble-solid interface of radius r [Fig. 2(d)].

Fig. 3(a) shows plots θ_b versus r in the range 1.5 to 3.5 mm for the four surfaces tested. In the case of the hydrophilic and hydrophobic surfaces, the value of θ_b reduces with reducing r whereas for the superhydrophobic surface the value of θ_b increases with reducing r. This latter observation appears to call into question a "line tension" explanation[17] for the effect, as the line tension should always act to reduce the contact angle for diminishing r.[24]

TABLE I. Experimental values of the liquid contact angle θ_l, the extrapolated bubble contact angle θ_{bi} at $h/R = 0$, and the measured slope α—the modeling values correspond to the bubble contact angle θ_{b0} (mod.) and the slope α (mod.).

	θ_l (exp.)	θ_{bi} (exp.)	α (exp.)	θ_{b0} (mod.)	α (mod.)
Black Si	111.9 (1.2)	132.3	−66.4	133.4	−66.8
Teflon	62.1 (2)	106.6	−50.7	108.2	−58.2
PDMS	52.8 (3)	102.4	−56.7	101.4	−57.7
SiO_2	9.6 (0.6)	90.2	−64.1	90.4	−58.9
Liquid	0	91.9	−170.4	90	−69.6

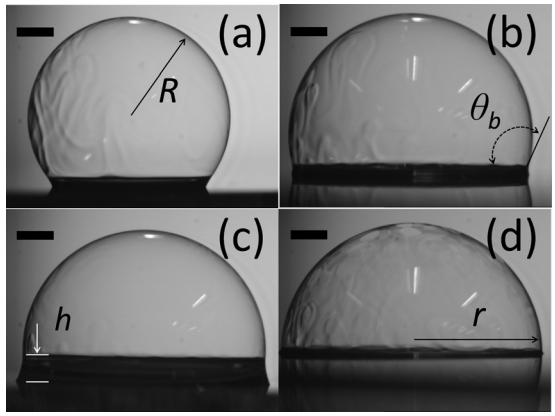

FIG. 2. Sessile bubbles wetting the solid surfaces used in the experiments. (a) Fluorocarbon coated "black silicon," (b) Teflon® AF coated silicon wafer, (c) PDMS, and (d) silicon dioxide. All scale bars = 1 mm. The parameters R (the curvature radius of the bubble), θ_b (the apparent contact angle of the bubble), h (the liquid film height), and r (the bubble base radius) are indicated.

Fig. 3(b) plots θ_b versus a dimensionless ratio of two lengths h/R associated with the bubble.[24] The standard deviation of the data points was determined to be 1.8°. For a given surface, the measured value of θ_b, corresponding to small values of h/R, increases from surfaces A to D. Also, as h/R increases the value of θ_b decreases, the data suggesting a near-linear relationship[19] for the four surfaces tested in the

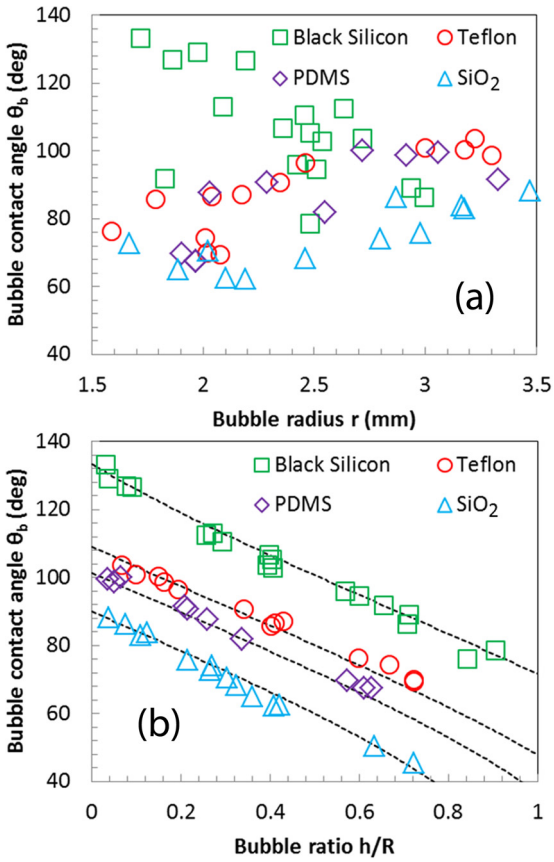

FIG. 3. A plot of the bubble contact angle θ_b versus the h/R ratio for the different surfaces tested. Fluorocarbon coated "black silicon" (open squares), Teflon® AF (open circles), PDMS (open diamonds), and silicon dioxide (open triangles). The dashed lines correspond to analytical solutions using Eq. (1) and Ref. 19.

range $h/R = 0$ to 0.7. A linear fit allows us to calculate the intercept bubble angle θ_{bi} using extrapolation. The value of θ_{bi} can be compared with the theoretical value of θ_{b0} predicted by Eq. (3) as $h/R \to 0$ (see Table I) within measurement error; the values compare well for all surfaces tested. A large variation of the bubble contact angle is observed here for the soap bubbles on superhydrophobic surfaces ($134° \to 76°$ (Fig. 3(b) open squares)) and on hydrophilic surfaces ($88.3° \to 45.4°$ (Fig. 3(b) open triangles)); the observations can be compared to those of Rodrigues *et al.*[17] who observed relatively small variations of the contact angle of a sessile soap bubble resting on a wet (~4°) and dry (<10°) surfaces and who invoked the controversial[24] line tension effect to explain their observations.

Equation (3) can explain the measured value of θ_{b0} as $h/R \to 0$, i.e., the wetting contact angle of an ideal bubble on a solid surface. However, in order to understand why θ_b decreases when h/R is increased we can implement a model[19] found in the literature for sessile bubbles wetting a solid surface. By using Eq. (3), when $h/R \to 0$, $\theta_b \to \theta_{b0}$, together with a first-order analytical solution which can be found in Ref. 19, we can compute the apparent contact angle of the bubble θ_b as a function of h/R for the various surfaces by using Eq. (4)

$$\cos\theta_b = \frac{1}{2}(\cos\theta_l - 1) + \frac{h}{R}. \tag{4}$$

The solutions [shown as dashed lines in Fig. 3(b)] correspond well with the experimentally obtained values of θ_b. The measured slopes, $\alpha = \mathrm{d}\theta_b/\mathrm{d}(h/R)$, correspond well to those predicted by the model (the near-linear range was taken to be $h/R = 0 \to 0.4$).

In terms of the bubble film thickness, no measurement of this was performed, but colours[6–8] are visible directly after bubble deposition indicating an initial film thickness in the sub-micrometer range;[24] drainage and evaporation produces black regions[6] (thickness < 10 nm)[24] where presumable the bubble first bursts[20] after a lifetime of seconds to tens of seconds. For an ideal bubble wetting a solid surface, the schematic diagram in Fig. 1(b) indicates an ideal bubble and that the film at the bubble-surface interface is continuous. However, Eqs. (2) and (3) simply imply that a single bubble surface needs to be created inside the bubble, i.e., the extra γ_l term on the *r.h.s.* of Eq. (3). Experimentally, as the sessile bubbles have a finite lifetime (~seconds to tens of seconds), bubble bursting[20] and its outcome can be observed. It was observed that one of two outcomes can be the result from bubble bursting: (i) The bubble bursts leaving a flat film of liquid (of radius r) which contracts into a well-defined spherical droplet having a contact angle θ_l and (ii) the bubble bursts resulting in a liquid ring of radius r.[20] This ring is observed to be unstable and either becomes a single droplet, suggesting a continuous film, or breaks-up into smaller droplets having a contact angle θ_l, presumably due to a Rayleigh-Plateau instability. Fig. 4 shows these outcomes for small values of h/R. In general for a large h/R ratio case (i) is observed. However as h/R reduces then bursting on a superhydrophobic and hydrophobic surface [Figs. 4(a) and 4(b)] results in a single droplet (indicating the presence of a continuous film at the bubble-solid interface

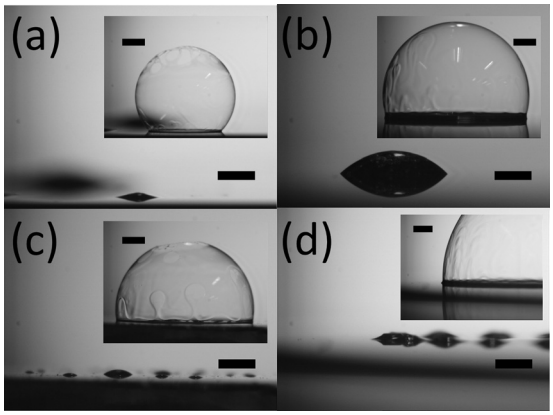

FIG. 4. Sessile bubbles bursting on solid surfaces. (a) Fluorocarbon coated "black silicon," (b) Teflon® AF coated silicon wafer, (c) PDMS, and (d) silicon dioxide. Insets show outcome of bursting. All scale bars = 1 mm.

even for small values of h/R) whilst bursting on a more hydrophilic film (PDMS and silicon dioxide) [Figs. 4(c) and 4(d)] results in an unstable liquid ring which stabilizes into a ring of droplets. The value of h/R for which the transition between forming a droplet after bursting and forming a ring of droplets after bursting was determined to be 0.245 (silicon dioxide) and 0.241 (PDMS). However, prior to bursting, it is important to note that the extrapolated values of θ_{bi} correspond very well to those values of θ_{b0} computed using Eq. (3).

Finally, let us now consider bubbles resting on the surface of a liquid as shown in Fig. 1(c). Fig. 5 shows sessile bubbles of differing sizes resting on the surface of a liquid composed of the same bubble solution. In general, the Plateau borders are larger—for a given bubble radius—than bubbles of the same size wetting a solid surface. The bubble contact angle is seen to diminish with bubble radius r. Fig. 6 shows a plot of θ_b versus bubble radius r. As r is varied from 10 mm to 645 μm, θ_b changes from 68.4° to 33.6°. A plot of θ_b versus h/R reveals itself to be linear [inset to Fig. 6], as is case with bubbles wetting the solid surfaces; the intercept θ_{bi} is 91.9° and the slope α is −170.4. The extrapolated intercept value of θ_{bi} is close to the 90° predicted by Eq. (3) assuming $\theta_l = 0$. In terms of sessile bubbles wetting a liquid film of the same liquid [Fig. 5], the value of α predicted by the model,[19] assuming a perfectly hydrophilic surface, does not correspond

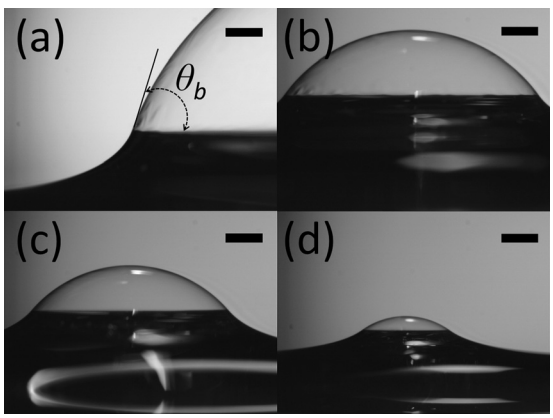

FIG. 5. Sessile bubbles of different base radii wetting a liquid film composed of the bubble solution. The contact angle of the bubble θ_b diminishes as the bubble base radius reduces (a) → (d). All scale bars = 1 mm.

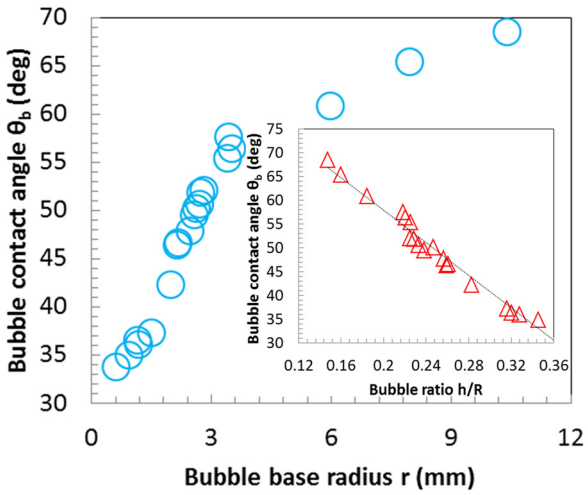

FIG. 6. A plot of the experimental bubble contact angle θ_b versus the bubble base radius r. Inset shows the straight line obtained when plotting the bubble contact angle θ_b versus the h/R ratio.

well with the experimental data for sessile bubbles wetting a liquid surface. Note that the experimental data for a hydrophilic surface given in Ref. 19 gives a slope α of $\sim$90. Although the data here suggest a near-linear relationship as is the case with bubbles wetting a solid surface [Fig. 3(b)], the measured slope corresponds is 2.4 times the value of α predicted for wetting on a perfectly hydrophilic surface. In other words, the data indicate that wetting behavior of a bubble on a perfectly hydrophilic solid surface is not the same as wetting of a bubble on a liquid film of the same liquid.

The author thanks Frank Hein (Pustefix) for discussions.

[1]P. Stevenson, *Foam Engineering: Fundamentals and Applications* (Wiley-Blackwell, 2012).
[2]A. Sylvester, T. Döring, and A. Schmidt, in *Proceedings of 4th International Conference on Tangible, Embedded, and Embodied Interaction*, 2010, p. 269.
[3]Y. Ochiai, A. Oyama, and K. Toyoshima, in Proceedings of SIGGRAPH Emerging Technologies, Los Angeles, California, 5–9 August 2012.
[4]G. Yu, A. Cao, and C. M. Lieber, Nat. Nanotechnol. **2**, 372 (2007).
[5]T. Georgiou, L. Britnell, P. Blake, R. V. Gorbachev, A. Gholinia, A. K. Geim, C. Casiraghi, and K. S. Novoselov, Appl. Phys. Lett. **99**, 093103 (2011).
[6]R. Hooke, *On Holes (Black Film) in Soap Bubbles* (Community Royal Society, 1672).
[7]I. Newton, *Opticks or a Treatise on the Reflections, Refractions and Inflections and the Colour of Light* (London, 1704).
[8]T. Young, Philos. Trans. R. Soc. London **92**, 387 (1802).
[9]J. A. F. Plateau, *Statique Expérimentale et Théorique des Liquides Soumis aux Seules Forces Moléculaires* (Ghent, 1873).
[10]J. Lyklema and K. J. Mysels, J. Am. Chem. Soc. **87**, 2539 (1965).
[11]M. Hutchings, F. Morgan, M. Ritoré, and A. Ros, Ann. Math. **155**, 459 (2002).
[12]R. E. Goldstein, H. K. Moffatt, A. I. Pesci, and R. L. Ricca, Proc. Natl. Acad. Sci. U.S.A. **107**, 21979 (2010).
[13]C. T. R. Wilson and G. I. Taylor, Proc. Cambridge Philos. Soc. **22**, 728–730 (1925).
[14]G. Taylor, Proc. R. Soc. London, A **280**, 383–397 (1964).
[15]O. Bonhomme, O. Liot, A.-L. Biance, and L. Bocquet, Phys. Rev. Lett. **110**, 054502 (2013).
[16]D. E. Moulton and J. A. Pelesko, J. Colloid Interface Sci. **322**, 252 (2008).
[17]J. F. Rodrigues, B. Saramago, and M. A. Fortes, J. Colloid Interface Sci. **239**, 577 (2001).
[18]P. I. C. Teixeira and M. A. Fortes, Phys. Rev. E **75**, 011404 (2007).
[19]M. A. C. Teixeira and P. I. C. Teixeira, J. Colloid Interface Sci. **338**, 193 (2009).
[20]J. Bird, R. de Ruiter, L. Courbin, and H. A. Stone, Nature (London) **465**, 759 (2010).
[21]U. Kornek, F. Müller, K. Harth, A. Hahn, S. Ganesan, L. Tobiska, and R. Stannarius, New J. Phys. **12**, 073031 (2010).
[22]Y. D. Afanasyev, G. T. Andrews, and C. G. Deacon, Am. J. Phys. **79**, 1079 (2011).
[23]T. Young, Philos. Trans. R. Soc. **95**, 65 (1805).
[24]P. G. de Gennes, F. Brochard-Wyart, and D. Quéré, *Capillarity and Wetting Phenomena* (Springer, 2004).
[25]R. J. Good and M. N. Koo, J. Colloid Interface Sci. **71**, 283 (1979).
[26]W. D. Harkins and F. E. Brown, J. Am. Chem. Soc. **41**, 499 (1919).
[27]B.-B. Lee, P. Ravindra, and E.-S. Chan, Chem. Eng. Commun. **195**, 889 (2008).
[28]S. Arscott, Sci. Rep. **1**, 184 (2011).
[29]M. Stubenrauch, M. Fischer, C. Kremin, S. Stoebenau, A. Albrecht, and O. Nagel, J. Micromech. Microeng. **16**, S82 (2006).
[30]M. K. Chaudhury and G. M. Whitesides, Langmuir **7**, 1013 (1991).